Journal of
Applied Remote Sensing

RemoteSensing.SPIEDigitalLibrary.org

Agreement analysis and spatial sensitivity of multispectral and hyperspectral sensors in detecting vegetation stress at management scales

Mikindra Morin
Rick Lawrence
Kevin Repasky
Tracy Sterling
Cooper McCann
Scott Powell

Mikindra Morin, Rick Lawrence, Kevin Repasky, Tracy Sterling, Cooper McCann, Scott Powell, "Agreement analysis and spatial sensitivity of multispectral and hyperspectral sensors in detecting vegetation stress at management scales," *J. Appl. Remote Sens.* **11**(4), 046025 (2017), doi: 10.1117/1.JRS.11.046025.

Agreement analysis and spatial sensitivity of multispectral and hyperspectral sensors in detecting vegetation stress at management scales

Mikindra Morin,[a,*] Rick Lawrence,[a] Kevin Repasky,[b] Tracy Sterling,[a] Cooper McCann,[c] and Scott Powell[a]

[a]Montana State University, Land Resources and Environmental Sciences Department, Bozeman, Montana, United States

[b]Montana State University, Electrical and Computer Engineering Department, Bozeman, Montana, United States

[c]Montana State University, Physics Department, Bozeman, Montana, United States

Abstract. Remotely sensed imagery is commonly used to map and monitor large land areas based on the ability to detect vegetation stress. Many sensors are available, including both hyper- and multispectral, but have varying costs, convenience, and characteristics. There were two objectives in this study: (1) to compare a hyperspectral sensor to two multispectral sensors with regards to each sensor's ability to detect vegetation stress indicators in the visible, red edge, near-infrared, and shortwave infrared portions of the spectrum and (2) to determine the ability of coarser-resolution sensors to detect stress indicators in areas, where a finer resolution sensor detected stress indicators. Pairwise agreements between the sensors were ~80% in each case, but much of this agreement was a function of agreement where stress indicators were absent. Spatial sensitivity analysis supported a conclusion that coarser-resolution sensors were consistently able to detect stress indicators in areas much smaller than their pixel size. [DOI: 10.1117/1.JRS.11.046025]

Keywords: spatial resolution; spectral resolution; Landsat; RapidEye; Pika II.

Paper 170340 received Jun. 3, 2017; accepted for publication Oct. 17, 2017; published online Dec. 19, 2017.

1 Introduction

1.1 *Relative Stress and Remote Sensing*

Plants, even if productive, are not generally growing under optimal conditions, because they are exposed to various stressors. Common stressors include water availability, low key nutrient levels, pathogens, and toxins. The stressors can vary, even over small distances and small amounts of time, such that, from a management perspective, relative stress is most relevant.[1] In other words, it is important to consider that two plants in close proximity and exposed to generally similar conditions might be presenting different levels of stress, so that management prescriptions might focus on locations exhibiting higher levels of stress, since all vegetation might theoretically be stressed at some level.

Monitoring the relative stress of plants in a particular area over time can provide important information about a large landscape. Mapping transient and persistent areas of relative stress and recognizing where changes in both are occurring can be a way to determine how the landscape is changing over time. Changes in areas where persistent relative stress is located might highlight certain issues that a land manager can then address to increase productivity, or alternatively, might indicate areas where site conditions are inherently limiting. Alternatively, locations exhibiting abrupt increases in stress might provide information related to changes in conditions that require more immediate attention.

---

*Address all correspondence to: Mikindra Morin, E-mail: mikindra.morin@gmail.com

1931-3195/2017/$25.00 © 2017 SPIE

Remote sensing, for decades, has been used to map vegetation stress over large land areas. It has been used in below-ground carbon dioxide leak detection,[2] nitrogen and water stress monitoring,[3] plant response to heavy metal toxicity,[4] mapping tree mortality,[5] and pipeline monitoring,[6] to name a few. Vegetation stress mapping has traditionally been conducted either using a supervised or unsupervised classification with the use of ground or airborne-based reference data. Given real-world limitations such as timing, inadequate resources, or limited access, however, obtaining reference data is not always feasible. Vegetation in areas with no reference data can still be mapped and monitored, however, based on the concept of relative stress. There are physiological differences between healthy and stressed vegetation, and these differences manifest themselves in the spectral response of plants.

1.2 *Physiological Sources of Reflectance Changes*

Vegetation has generally been said to respond in the same way spectrally regardless of the source of environmental stress.[7–9] These changes can be detected remotely as early as 16 days before visible signs of stress are detectable,[7,10,11] making it a useful monitoring tool. Physiological changes in vegetation due to stress result in specific changes in the visible, red edge, near-infrared (NIR), and shortwave infrared (SWIR) portions of the spectrum.

Leaf pigments are the primary absorbers of light in plants in the visible portion of the spectrum, from 400 to 700 nm.[8,12] Chlorophyll is the key absorber, but carotenoids, xanthophylls, and anthocyanins also have an absorptive effect.[12] Stress causes a reduction in leaf pigments either due to stress-induced pigment deterioration or impairment in pigment biosynthetic pathways.[13] This reduction, therefore, results in an increase in visible reflectance (Table 1).

The NIR portion of the spectrum, 750 to 1000 nm, experiences a decrease in reflectance due to stress because of changes in the internal structure of plant cells.[12,14] NIR reflectance is high in healthy vegetation because of the intercellular spaces and internal scattering caused by cell walls. Cell walls begin to collapse and mesophyll cells shrink as stress increases, resulting in less intercellular space and cellular surface area and a decrease in NIR reflectance[15] (Table 1).

The red edge, 680 to 740 nm, reflectance response to vegetation is a result of the sharp increase in reflectance between the low red reflectance, due to chlorophyll absorption, and the high NIR reflectance caused by internal leaf scattering.[16] An increase in the reflectance in red edge wavelengths is an early indicator of stressed vegetation[17–19] (Table 1).

Water generally absorbs strongly in the SWIR portion of the spectrum, 1000 to 2500 nm.[20] Leaf water content generally decreases as vegetation stress increases. Stressed vegetation, therefore, has a higher SWIR reflectance than healthy vegetation[15] (Table 1).

This information (Table 1) allows for the creation of stressed vegetation indicator maps by locating anomalies in any of the aforementioned spectral regions. It is expected that vegetation located in a similar area, i.e., having similar soil and climate, that is also managed similarly, will have a similar spectral response; although, within a management area, species or other variability are likely to still exist as confounding factors. A pixel that is exhibiting a spectral response that is outside a predetermined range for a pixel in close proximity and with the same management

Table 1 Summary of the stress rules that are the basis of our spectral analyses herein.

Spectrum portion	Stress rule	Reflectance response	Physiological source
Visible	vis-rule	Increased reflectance	Reduction of photosynthetic pigments, the main source of absorption in this portion of the spectrum
NIR	NIR-rule	Decreased reflectance	Collapse of cell walls and shrinkage of mesophyll cells—resulting in less intercellular space and cellular surface area
Red edge	edge-rule	Increased reflectance	Change in the visible reflectance, due to chlorophyll absorption, and the NIR reflectance, due to internal leaf scattering
SWIR	SWIR-rule	Increased reflectance	Decrease in leaf water content

practices can be defined as an anomaly and potential area of stress that might warrant further investigation.[21] One example of a circumstance, and the driver of this study, where mapping the relative stress of an area using remote sensing could be a valuable tool is in monitoring geologic carbon sequestration areas by mapping indicators of vegetation stress. Carbon sequestration areas are often quite large, have access issues due to multiple landowners, and are necessary to monitor because of the importance of detecting a leak quickly and efficiently.

1.3 *Sensors Used in this Study*

A variety of remote sensing instruments and data products are available with a wide range of spatial and spectral characteristics. Determining which remote sensing instrument or data product to use is based on the desired remote sensing application, availability, and cost of data acquisition. The overarching goal of this study was to compare the agreement in detecting vegetation stress indicators between three sensors with varying characteristics. The indicators are based on decades of remote sensing research determining the spectral differences between healthy and stressed vegetation. They are not necessarily determinative of vegetation stress (i.e., a spectral indicator of stress does not guarantee the existence of stressed vegetation) but might be indicative of areas that warrant further investigation in a monitoring scheme.

The sensors that were used in this study included the operational land imager (OLI) aboard the Landsat 8 satellite,[22] the multispectral sensor aboard RapidEye (Satellite Imagine Corporation, Houston, Texas), and a commercial flight-based hyperspectral sensor (Pika II from Resonon, Inc., Bozeman, Montana). These sensors have many differing characteristics and represent, in many cases, the range of capabilities available in airborne and space-borne sensors for moderate- to fine-scale vegetation monitoring.

Landsat 8 is a satellite that has been in orbit since 2014 and carries the OLI with nine bands ranging from the visible to the SWIR (Landsat 8's Thermal Infrared Sensor was not used for this study). It has 30-m spectral resolution and a return interval of 16 days. The images are available free of charge through the United States Geological Survey (USGS) Landsat archive (earthexplorer.usgs.gov) (Table 2).

The RapidEye constellation of satellites is owned by the Blackbridge Group. It is a multispectral sensor with 5-m spatial resolution and five bands ranging from the visible to the NIR. It has a red edge band that is specifically designed for vegetation characterization. RapidEye has an off-nadir daily revisit time and a 5.5 day at nadir revisit time. The images can be purchased from the Blackbridge Group. Cost varies depending on numerous factors; the imagery acquired for this study cost \$3605 (Table 2).

The Pika sensor is a hyperspectral sensor sold by Resonon Inc.[27] It has 80 bands ranging from the visible to the NIR and a spatial resolution that varies depending on flight altitude (1 m for this study). The instrument is mounted in a plane and flown over the area of interest, which allows for a flexible revisit time (Table 2).

1.4 *Study Objectives*

The overarching objective of this study was to evaluate the extent to which these vastly different sensors might agree or disagree in their detection of indicators of vegetation stress. Based on the literature reviewed above, stressed vegetation should exhibit one or more indicators listed in Table 1, and therefore, indicators of stress from these very different sensors should agree in terms of spatial location and distribution. Failure of these sensors to so agree would indicate that the choice of sensor might be critical for monitoring vegetation stress for either research or operational purposes. We took two approaches to evaluating the level of this agreement or disagreement. The first was to compare the agreement between these three sensors in their ability to detect spectral indicators of vegetation stress. It is important to understand, given their different characteristics, how well they detect stress compared to each other so that decisions can be made regarding, which is most appropriate in individual monitoring schemes. The second objective was to analyze the spatial sensitivity of the lower-resolution sensors as compared to the higher-resolution sensors. This analysis might assist in determining, if a given area threshold is relevant for a manager, whether coarser-resolution imagery might be adequate for the given application. For example, if Landsat consistently detected a stress indicator when only

Table 2 Overview of the three sensors used in this study.

Characteristic	Landsat[a]	RapidEye[b]	Pika[c]
Spatial resolution (m)	30	5	1
Spectral range	Visible: Coastal blue: 430 to 450 nm Blue: 450 to 510 nm Green: 530 to 590 nm Red: 640 to 670 nm NIR: 850 to 880 nm SWIR: 1570 to 1650 nm 2110 to 2290 nm Panchromatic: 500 to 680 nm Cirrus: 1360 to 1380 nm Thermal: 10,600 to 11,190 nm 11,500 to 12,510 nm	Visible: Blue: 440 to 510 nm Green: 520 to 590 nm Red: 630 to 685 nm Red edge: 690 to 730 nm NIR: 760 to 850 nm	425 to 925 nm
Applicable rules	vis-rule NIR-rule SWIR-rule	vis-rule edge-rule NIR-rule	vis-rule edge-rule NIR-rule
Spectral resolution	11 bands	5 bands	80 bands
Revisit time	16 days	Daily (off-nadir) 5.5 days (at nadir)	Variable, flights are scheduled by user
Cost	Free	Order images Costs vary	Cost of sensor and additional costs for flights
Signal-to-noise ratio (SNR)	150 to 360 (range)	50 to 150 (range)[23]	198 (max)
Quantization (bit)	12	12	12

[a]Department of the Interior, Landsat 8 (L8) Data Users Handbook (2016).[24]
[b]Satellite Imaging Corporation[25] (except signal-to-noise).
[c]Resonon.[26]

100 of 900 of the Pika pixels within that Landsat pixel detected a stress indicator, then Landsat might be able to detect stress indicators at a scale of 100 m^2, rather than 900 m^2.

2 Methods

2.1 *Study Area*

The study area for this work is located in northcentral Montana at the big sky carbon sequestration partnership site[28] located ∼24 km north of Shelby, Montana (Fig. 1). There are three separate study sites within the larger study area. The larger study site is used primarily for non-irrigated row crops, growing wheat and barley, unmanaged grass/shrubland, and small areas used for domestic purposes. None of the domestic areas are located within our three study areas.

2.2 *Image Acquisition*

Five images were used in this study. The Landsat image, acquired July 12, 2014, was obtained from the USGS Landsat archive and encompasses all three study sites. This image was chosen because it is devoid of clouds and was near the date of the hyperspectral flight. The RapidEye image, from June 18, 2014, was purchased through Apollo Mapping of Boulder, Colorado, pursuant to a task order for our study location and also encompasses all three study sites. The hyperspectral flight occurred on June 20, 2014, and resulted in three images. A Pika II hyperspectral sensor was mounted into a viewhole in the fuselage of a single engine Cessna Skyhawk airplane, which was flown at 1200 m over the study area and resulted in 1-m pixel sizes. The original images were radiometrically referenced to one another and mosaicked to produce three radiometrically consistent hyperspectral images.[29]

2.3 *Analysis*

The objective of this study was to compare the number of stress indicators present in each pixel in similarly managed areas across all three sensors. A set of stress indicator rules was developed based on the known physiological differences between healthy and stressed vegetation (Table 1). Images were then subset by management regime and evaluated based on these stress indicator rules.

Each of the three study sites contained seeded, fallow, and unmanaged areas. We would expect vegetation within each of these management regimes to have similar spectral responses. We, therefore, cropped each of the Landsat, RapidEye, and Pika images based on these

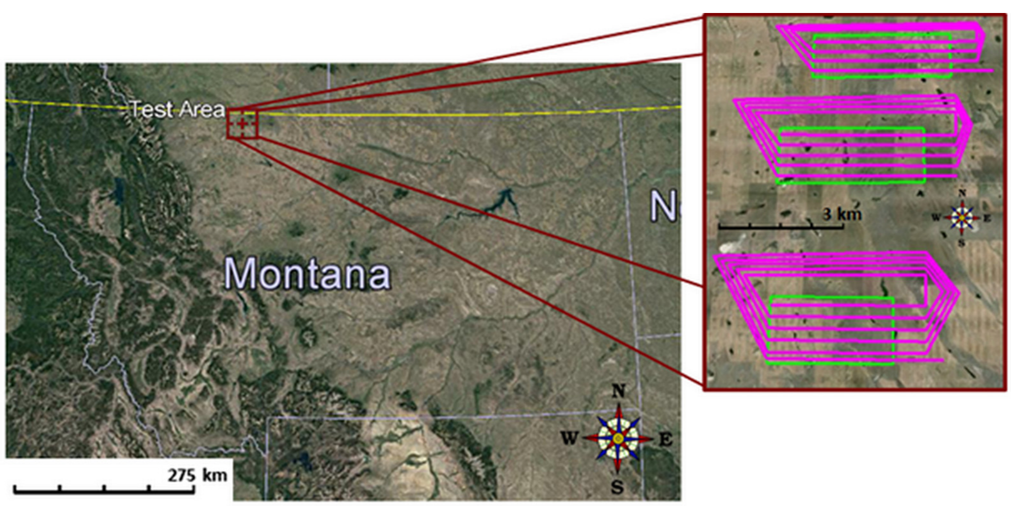

Fig. 1 Study site in northern Montana with the flight paths for the hyperspectral images. The three separate study sites within the larger study area are outlined in green.

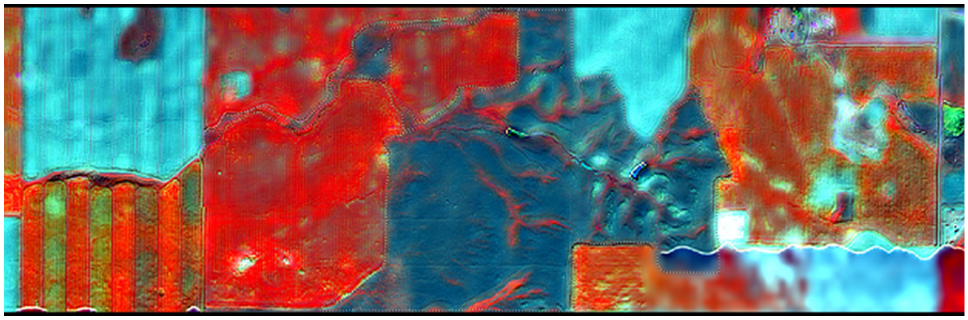

Fig. 2 The hyperspectral image used to determine appropriate management areas, displayed in as a standard false color composite. Interpretation followed three general guidelines: (1) seeded areas appear as relatively uniform red (e.g., lower left red strips and middle left block), (2) fallow areas appear as uniform cyan (e.g., upper left) or, in areas where there is strip cropping, greenish areas between seeded, red strips (e.g., lower left green strips), and (3) the unmanaged areas are those appearing as nonstripped, nonuniform colors (e.g., upper right area of mixed red, cyan, and blue).

management practices by creating a false color Pika image and visually interpreting where each use was being practiced throughout the study area (Fig. 2). We created shapefiles, buffering the edges to avoid mixed pixels, for each management practice in each of the three study areas. This resulted in nine separate images per sensor, 27 total, to be used in this study.

The goal, once management areas were defined, was to detect areas that were spectrally consistent with signs of stressed vegetation based on stress indicators (Table 1). An anomaly was defined as being a certain standard deviation from the mean for a given management area within an image. A high anomaly in any of the visible bands would be considered a stress indicator. We generated images at 1, 1.5, and 2 standard deviations from the mean (Fig. 3). Visual interpretation was used to determine that 1.5 standard deviations was an appropriate value to define an anomaly for the goals of this study. A standard deviation of 1.5 is neither over- nor under-inclusive of vegetation outside the norm for a study area with similar vegetation, as seen previously.[21] The standard deviation can be altered based on individual management goals that might require more or less inclusiveness.

We formulated a set of stress indication rules (Table 1) based on the aforementioned research documenting vegetation's spectral response to stress. A stress indicator was defined as a high visible anomaly (vis-rule), a low NIR anomaly (NIR-rule), a high red edge anomaly (edge-rule), or a high SWIR anomaly (SWIR-rule). A map of relative stress within management zones using these stress indicators was created for each of the 27 images. We reclassified each pixel based on the number of stress indicators that were detected.

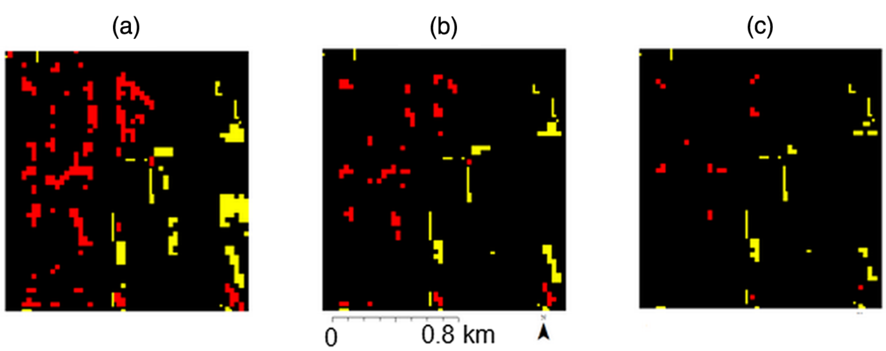

Fig. 3 Landsat NIR anomaly maps of the cropped management zone of the southernmost portion of the study area. High anomalies are displayed in red, and low anomalies are displayed in yellow. (a) Anomalies 1 standard deviation above or below the mean. (b) Anomalies 1.5 standard deviations above or below the mean. (c) Anomalies 2 standard deviations above or below the mean.

2.3.1 *Agreement analysis*

We had two avenues of analysis in this study. The first was to evaluate the absolute agreement between the sensors based on whether the coarser spatial resolution image showed the same number of stress indicators as the finer spatial resolution image in each pixel (i.e., if a Landsat pixel exhibited three stress indicators and any RapidEye pixel within the Landsat pixel also exhibited three stress indicators, the sensors were judged to be in agreement for the location occupied by the Landsat pixel). The output for this analysis was a series of tables. These tables compared overall agreement between two sensors (i.e., where there was full agreement as in the example above) and also where the sensors showed a different numbers of stress indicators (e.g., where the Landsat pixel exhibited three stress indicators but no RapidEye pixel within the Landsat pixel exhibited more than two stress indicators). This analysis demonstrated, across scales, the relative spatial agreement of the sensors to detect spectral indicators of vegetation stress.

2.3.2 *Spatial sensitivity analysis*

The second avenue of analysis was a sensitivity analysis to determine how many pixels where stress indicators were detected in the higher spatial resolution image were contained within each pixel of the coarser spatial resolution image. For each coarser spatial resolution pixel showing at least one stress indicator, the number of finer resolution pixels contained within that pixel also detecting at least one stress indicator was calculated. We then generated a histogram showing, within the coarser-scale pixel detecting at least one stress indicator, the area occupied by finer-scale pixels detecting at least one stress indicator. This analysis provided an indication of the coarser-resolution imagery's ability to detect subpixel indicators of stress that were detected by the finer-resolution imagery.

3 Results

The general spatial distribution of stress indicators, including the number of stress indicators, was similar for all sensors, based on a qualitative visual inspection of the results (Fig. 4). In this image of the seeded portion of the northernmost study area, the pocket of stress in the southeast corner exhibits the highest concentration of stress indicators for all three sensors, as do patterns associated with strip cropping in the western portion of the images. As spatial resolution increased, however, there was an increase in the detection of small areas containing stress indicators that were not observed at coarser resolutions. This detection of smaller areas exhibiting signs of stress is noticeable throughout the entire Pika/RapidEye images, but especially in the fields in the western portion of the image when compared to the Landsat image.

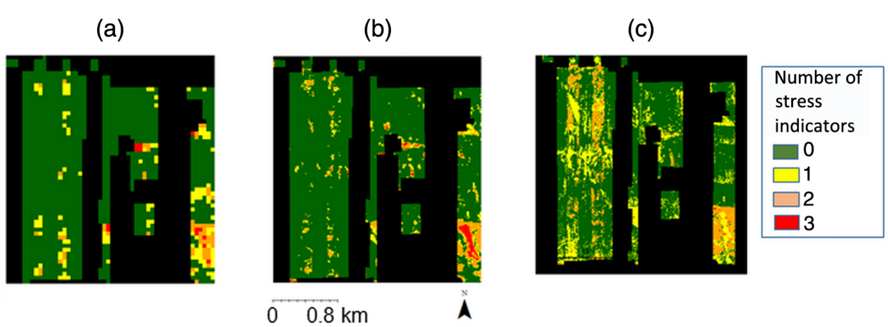

Fig. 4 Stress indicator maps of seeded field from (a) Landsat, (b) RapidEye, and (c) Pika sensors. Green areas indicate areas with no stress indicators present, yellow areas are instances of one stress indicator, orange areas are instances of two stress indicators, and red areas are instances of three stress indicators.

Table 3 Agreement analysis, based on the number of stress indicators detected (0, 1, 2, or 3), between Landsat and RapidEye sensors.

		RapidEye					% RapidEye agrees with Landsat
		0	1	2	3	Total	
Landsat	0	504,854	19,866	8535	670	533,925	94.56
	1	16,249	7561	4298	270	28,378	26.64
	2	5679	2798	9555	1015	19,047	50.17
	3	456	272	1160	1433	3321	43.15
	Total	527,238	30,497	23,548	3388		
% Landsat agrees with RapidEye		95.75	24.79	40.58	42.30		
% Landsat and RapidEye agree overall			89.52	Kappa	0.39		

3.1 *Agreement Analysis*

The culmination of the agreement analysis was a set of tables (Tables 3, 4, and 5) comparing the overall agreement between the sensors and also the agreement between the number of stress indicators in each pixel. The overall agreement between each sensor comparison is shown at the bottom of this table. This number indicates the percentage of pixels in the images that detected the same number of stress indicators, ranging between zero (no anomalies) to three. Using Table 3 as an example, the tables should be read in the following way: The "% RapidEye agrees with Landsat" column indicates, for one Landsat pixel, how often RapidEye detected the same number of stress indicators as Landsat. For example, 50.17% of the pixels where Landsat detected two stress indicators, RapidEye also detected two stress indicators. This number was calculated by dividing the number of pixels in agreement (9555) by the total number of pixels in which Landsat detected two stress indicators (19,047). The "% Landsat agrees with RapidEye" row is read in a similar manner. It determines, where RapidEye detects a certain number of stress indicators, how often Landsat detects the same number of stress indicators. Therefore, 40.58% of

Table 4 Agreement analysis, based on the number of stress indicators detected, between RapidEye and Pika sensors.

		Pika					% Pika agrees with RapidEye
		0	1	2	3	Total	
RapidEye	0	10,979,028	176,0129	510,299	19,217	13,268,673	82.74
	1	503,899	203,565	69,827	2499	779,790	26.11
	2	302,051	114,697	151,125	4911	572,784	26.38
	3	32,514	2448	23,299	3333	61,594	5.41
	Total	11,817,492	208,0839	754,550	29,960		
% RapidEye agrees with Pika		92.90	9.78	20.03	11.12		
% RapidEye and Pika agree overall			77.21	Kappa	0.13		

Table 5 Agreement analysis, based on the number of stress indicators detected, between Landsat and Pika sensors.

		Pika					% Pika agrees with Landsat
		0	1	2	3	Total	
Landsat	0	11,103,505	1,718,325	480,892	15,151	13,317,873	83.37
	1	390,671	224,990	89,615	2498	707,774	31.79
	2	197,097	126,582	148,604	25,177	497,460	29.87
	3	22,053	30,913	25,175	5905	84,046	7.03
	Total	11,713,326	2,100,810	744,286	48,731		
% Landsat agrees with Pika		94.79	10.71	19.97	12.12		
% Landsat and Pika agree overall			78.61	Kappa	0.18		

the pixels where RapidEye detected two stress indicators, Landsat did as well. Again, this number is calculated by dividing the number of times both RapidEye and Landsat detected two stress indicators (9555) by the total number of pixels where RapidEye detected two stress indicators (23,548). This same analysis was done for Tables 3 and 4 as well.

The overall agreement, calculated by determining the number of pixels that were in agreement and dividing that by the total number of pixels in the image, was highest in the Landsat/RapidEye comparison (89.52%) (Table 3) but was still relatively high for the Landsat/Pika comparison (78.61%) and the RapidEye/Pika comparison (77.21%). Most of the agreement can be attributed to areas where no stress indicators were detected in either sensor. In the RapidEye/Landsat comparison, 94.56% of the pixels where Landsat did not detect any stress indicators, RapidEye did not either, and 95.75% of the pixels where RapidEye detected no stress indicators, Landsat did not either (Table 3). Agreement percentages decreased drastically for pixels where at least one stress indicator was detected. In the same RapidEye/Landsat comparison, less than half (40.58%) of the pixels where RapidEye detected two stress indicators did Landsat also detect two stress indicators and in only 12.09% of the pixels where Landsat detected two stress indicators did RapidEye also detect two indicators (Table 3).

The agreement in areas where both RapidEye and Landsat sensors detected all three stress indicators was 43.15% and 42.30%, respectively, but it was quite low in the other instances. The opposite is true in the Pika/RapidEye comparison (Table 4). Agreement percentage declined as one sensor detected a larger number of stress indicators. Where RapidEye detected all three stress indicators, Pika only detected three indicators in 5.41% of those pixels. The Landsat/Pika sensors also showed low agreement in pixels where one sensor detected all three stress indicators (7.03% of the pixels where Landsat detected all three stress indicators) but agreed more frequently where one or two indicators were detected (31.79% where Landsat detected one stress indicator) (Table 5).

We further explored graphically (Fig. 5) the level of agreement/disagreement among the sensors where the coarser-resolution sensor detected no stress indicators, since these pixels were driving the overall agreement results. This graph shows that when a coarser-resolution sensor detected no stress indicators within a pixel, the majority of the time the finer resolution sensor also detected no stress indicators within that same land area. When Landsat detected no stress indicators within a 30-m pixel ∼70% of the time, RapidEye detects stress in less than 5% of that land area as well.

We also evaluated the level of agreement for detecting any stress indicators, as opposed to the number of stress indicators detected. This approach potentially loses information with respect to the likelihood that stress is present (e.g., if three stress indicators are present, it is more likely that

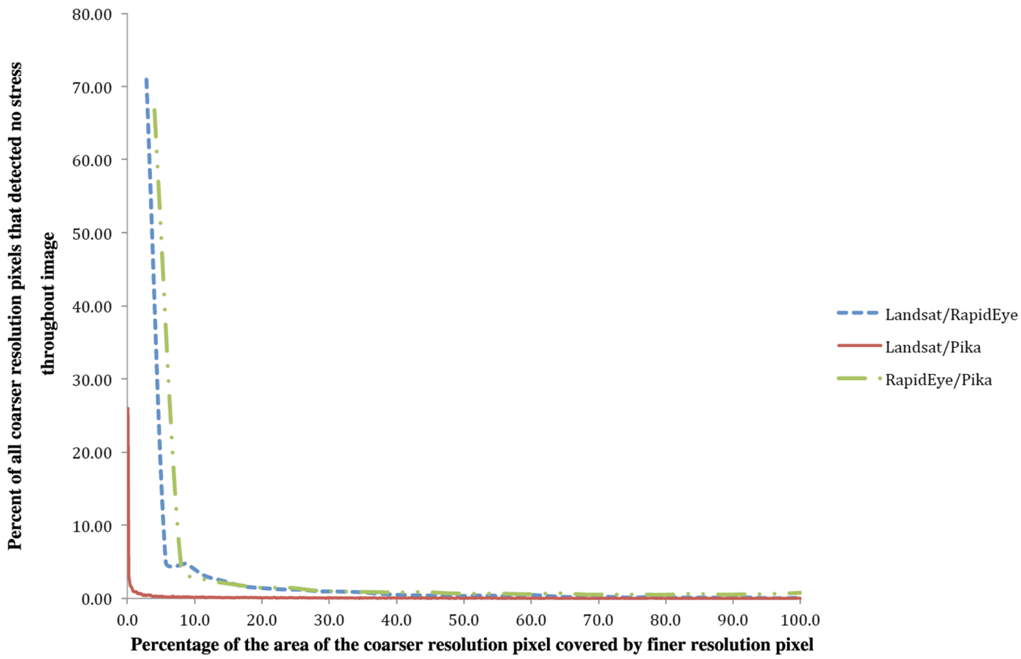

Fig. 5 Graph depicting, within a coarser-resolution pixel detecting no stress indicators, the percent area of finer-resolution pixels detecting at least one stress indicator.

vegetation stress is present than if only one indicator is present) but avoids potential confusion caused by the sensors having different indicators of stress (e.g., Landsat does not have a red edge indicator, whereas RapidEye and Pika do not have SWIR indicators).

These tables (Tables 6, 7, and 8) can be read similarly to the ones above (Tables 3, 4, and 5). The overall agreement again indicates the percentage of pixels where the sensors agreed. Contrary to the above tables, however, the sensors do not have to have agreement on the specific number of stress indicators to qualify as pixel agreement. In these tables, "no stress" is defined as a pixel where no stress indicators were detected, and "stress" is defined by at least one stress indicator (either 1, 2, or 3) being detected in a pixel. Using Table 6 as an example, the "% Landsat agrees with RapidEye" row indicates the percentage of times Landsat detected either stress or no stress when RapidEye did. For example, 49.38% of the pixels where RapidEye detected at least one stress indicator, Landsat did as well. This is calculated by dividing the total number of pixels where both Landsat and RapidEye detected at least one stress indicator (28,362) by the total number of pixels where RapidEye detected at least one stress indicator

Table 6 Agreement analysis, based on whether any stress indicators were detected, between Landsat and RapidEye sensors. Numbers under "no stress" and "stress" indicate number of pixels detecting any or no indicators of vegetation stress.

		RapidEye			% RapidEye agrees with Landsat
		No stress	Stress	Total	
Landsat	No stress	504,854	29,071	533,925	94.56
	Stress	22,384	28362	50,746	55.89
	Total	527,238	57,433		
% Landsat agrees with RapidEye		95.75	49.38		
% Landsat and RapidEye agree overall			91.20		

Table 7 Agreement analysis, based on whether any stress indicators were detected, between RapidEye and Pika. Numbers under "no stress" and "stress" indicate number of pixels detecting any or no indicators of vegetation stress.

		Pika			
		No stress	Stress	Total	% Pika agrees with RapidEye
Landsat	No. stress	10,979,028	2,289,647	13,268,675	82.74
	Stress	829,464	638,614	1,468,078	43.50
	Total	11,808,492	2,928,261		
% RapidEye agrees with Pika		92.98	21.81		
% Pika and RapidEye agree overall			78.83		

Table 8 Agreement analysis, based on whether any stress indicators were detected, between Landsat and Pika. Numbers under "no stress" and "stress" indicate number of pixels detecting any or no indicators of vegetation stress.

		Pika			
		No stress	Stress	Total	% Pika agrees with Landsat
Landsat	No stress	10,103,505	2,214,368	12,317,873	82.02
	Stress	609,821	660,126	1,269,947	51.98
	Total	10,713,326	2,874,494		
% Landsat agrees with Pika		94.31	22.96		
% Landsat and Pika agree overall			79.20		

(57,433). The "% RapidEye agrees with Landsat" column can be read similarly. It indicates, where Landsat detects no or at least one stress indicator, how often RapidEye detects the same. For example, 55.89% of the pixels where Landsat detects at least one stress indicator, RapidEye also detects at least one stress indicator. This number is calculated by dividing the number of pixels where both Landsat and RapidEye detect at least one stress indicator (28,362) by the total number of pixels where Landsat detected at least one stress indicator (50,746).

These tables also demonstrated a high level of overall agreement. The Landsat/RapidEye comparison (Table 6) again had the highest agreement percentage (91.20%), but the Pika/RapidEye (78.83%) (Table 7) and Pika/Landsat (79.20%) (Table 8) comparisons were also relatively high. The high level of agreement again is largely attributable to pixels where no stress indicators were detected by either sensor.

The Landsat/RapidEye comparison (Table 6) had the highest agreement outside of the pixels where no stress indicators were detected but not substantially. Both comparisons with the Pika sensor (Tables 7 and 8) were similar in that both had a percentage of finer-resolution pixels agreeing with coarser-resolution pixels around 50% (43.50% and 51.98%) and a percentage of coarser-resolution pixels agreeing with finer-resolution pixels around 20% (21.81% and 22.96%). This means that in pixels where Landsat or RapidEye detected a stress indicator, Pika was about 50% likely to also detect a stress indicator. In pixels where Pika detected a stress indicator, though, Landsat or RapidEye were only about 20% likely to also detect a stress indicator.

3.2 *Spatial Sensitivity Analysis*

The output for the sensitivity analysis was a histogram (Fig. 6). This histogram showed, when a coarser-resolution pixel detected at least one stress indicator, the percentage of that land area that the finer-resolution sensor also detected at least one stress indicator. For example, for one Landsat pixel that is 30 m × 30 m, what percentage of RapidEye pixels, which each cover ∼3% of a Landsat pixel, also detected at least one stress indicator. The histogram can be interpreted in the following way (Fig. 6): using the example of the second vertical bar, for ∼18% of all of the Landsat pixels that detected at least one stress indicator within the image, 0% to 10% of the land area covered by RapidEye pixels also detected at least one stress indicator.

All three comparisons show a similar trend, with a spike at 0% to 10% or less and an additional spike at 91% to 100%. The large percentage of instances where the finer-resolution sensor detected no stress indicators on at least 90% of the land area where the coarser-resolution sensor detected a stress indicator (the left three vertical bars) was unexpected and warranted further analysis. We, therefore, did a pixel-by-pixel breakdown of those occurrences.

The largest number of the Landsat pixels that detected at least one stress indicator contained 36 RapidEye pixels (the entire number of RapidEye pixels within a Landsat pixel) also detecting at least one stress indicator (Fig. 6). There are, however, 140 instances where a Landsat pixel detected signs of stress and none of the RapidEye pixels within the Landsat pixel detected a stress indicator. There were 147 stress indicators detected by Landsat within these 140 pixels. Twenty-two (15.0%) were instances where Landsat detected a high visible anomaly, 82 (47.1%) were low NIR anomalies, and 43 (29.3%) were high SWIR anomalies.

Pika is likely to detect at least one stress indictor in all 900 pixels of a Landsat pixel also detecting at least one stress indicator (Fig. 6). There is a relatively large number (105) of pixels, however, in which Landsat detected at least one stress indicator and there were zero Pika pixels detecting stress indicators in that same pixel, similar to the results seen in the Landsat/RapidEye comparison. Of the 130 stress indicators in these 105 pixels, 39 (30%) were in the visible portion of the spectrum, 51 (39.2%) were in the NIR, and 40 (30.8%) were in the SWIR.

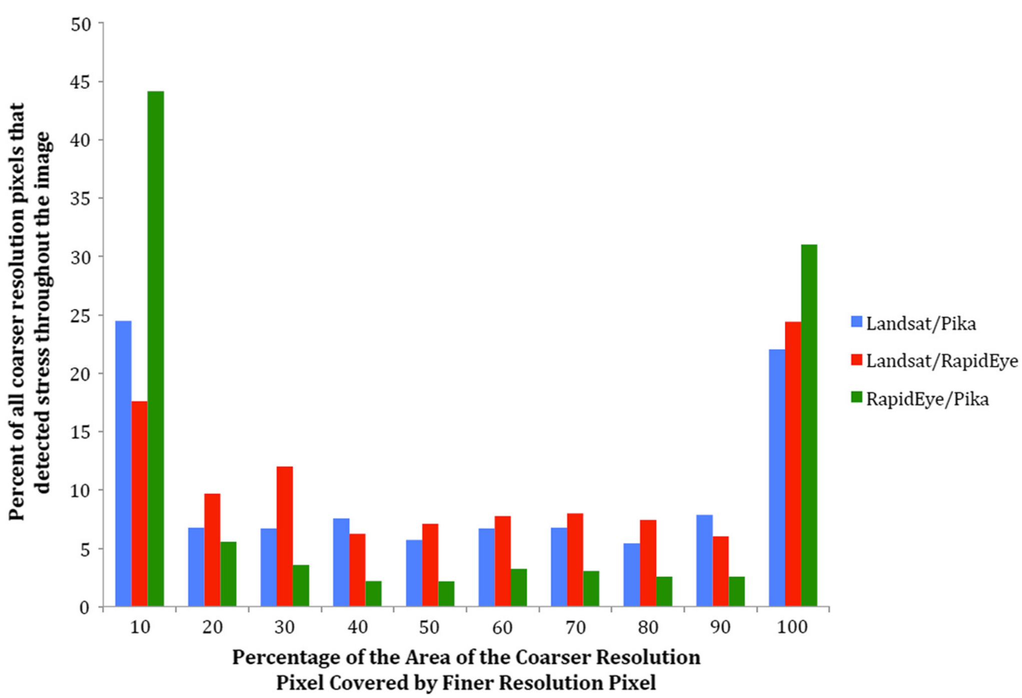

Fig. 6 Graph depicting the percentage of land area, when a coarser-resolution pixel detects a stress indicator, that the finer resolution pixel also detects a stress indicator.

The most significant difference between the RapidEye/Pika sensitivity analysis and the others is that of the roughly 40,000 RapidEye pixels detecting at least one stress indicator, in 15,000 instances all 25 Pika pixels within that pixel also detected at least one stress indicator, but in $\sim$21,000 of those pixels, more than half, there are zero Pika pixels that detected at least one stress indicator (Fig. 4). There were 35,919 stress indicators that RapidEye detected in these 21,000 pixels. Of those, 14,959 (41.65%) were in the visible portion of the spectrum, 9486 (26.41%) in the red edge, and 11,474 (31.94%) in the NIR.

4 Discussion

4.1 *Agreement Analysis*

It is important, when using remotely sensed data, to remember that sensors are each different and are, therefore, able to detect vegetation in different ways. The three sensors used in this study have different specifications (Table 2) that contribute to their ability to detect vegetation stress.

4.1.1 *Areas of substantial agreement*

The overall agreement between the three sensors was quite high. Most of this agreement can be attributed to areas where no stress indicators were detected by any sensors. This is not surprising given that we expect similarly situated and treated vegetation to have a similar spectral response. The general spatial locations of stress indicators also demonstrated a high level of agreement (Fig. 4).

4.1.2 *Areas of substantial disagreement*

Precise agreement of the location of stress indicators, however, was relatively low, especially when analyzing agreement with the Pika sensor. Disregarding areas where no stress indicators were present, which accounted for the high percentage of overall agreement, the agreement between sensors on the number of stress indicators present in each pixel dropped dramatically (Tables 3, 4, and 5). This is also reflected in the Kappa statistics for the full matrixes, which were low, indicating that there was substantial potential that chance agreement accounted for a substantial portion of the accuracy. The collapsed agreement tables, which analyzed the level of agreement when at least one stress indicator was present, did increase agreement in this area, but it was still below 50% (Tables 6, 7, and 8). We believe there were two primary factors resulting in this level of disagreement, spatial and spectral resolution, as discussed below.

4.1.3 *Number of indicators present*

An important revelation of this study was that many pixels that detected a stress indicator did not detect all three. The reflectance differences associated with vegetation stress might be expected to coexist, because the physiological changes associated with stress coexist. The reflectance changes, however, do not always occur at the same rate or begin at the same time. The red edge, for instance, is a good stress indicator in the early stages of stress but will eventually return to its healthy vegetation value.[30] The increase in reflectance in the SWIR portion of the spectrum due to a decrease in leaf water content only manifests when the water content has decreased to extreme water stress levels,[7] which might not occur until much later than the visible, red edge, and NIR differences can be detected. The red and NIR portions of the spectrum are commonly used to detect vegetation stress, such as with the normalized difference vegetation index. The physiological changes in stressed vegetation do not always occur at exactly the same time or at the same rate, however.[31] The reflectance changes, therefore, also do not always occur at the same time or rate. This indicates the need, at least with respect to detection of vegetation stress, for sensors that include both red edge and SWIR capabilities to best detect both early and late vegetation stress. None of the sensors tested in this study contained both capabilities.

The sentinel 2 satellites (European Space Agency) include both capabilities but were not available at the time of this study.

4.2 *Potential Sources of Disagreement in this Study*

There are a multitude of possible explanations for the disagreement among the sensors as to whether stress indicators were present and, if so, where. One source of potential disagreement was the spatial accuracy of the sensors. After GPS/INU correction and manual georeferencing, an root mean square error of 3 to 5 m for ground control points was reached (although accuracy for nonground control points might be worse) while Landsat generally has a spatial accuracy of at least 12 m.[32] Therefore, there were likely disagreements among the sensors resulting solely from spatial offsets, although these could not be quantified. Another unquantifiable source of potential disagreement was atmospheric effects. All data used in this study was at sensor. The Pika sensor, specifically, will be less affected by atmospheric effects than the Landsat or RapidEye sensors because of the Pika's platform low flight elevation. The two primary potential sources of disagreement that were explored in this study were spatial and spectral resolution.

4.2.1 *Spatial resolution*

There are dramatic spatial resolution differences among these three sensors. Landsat has 30-m resolution, RapidEye has 5-m resolution, and Pika has 1-m resolution. This difference results in RapidEye and especially Pika having the capability to detect much smaller areas containing stress indicators. One very noticeable example of this was when examining all three images side-by-side. The higher resolution images detected stress in much smaller areas throughout the image (Fig. 4).

4.2.2 *Spectral differences*

There are spectral differences among these three sensors as well, both in the number of bands and in the portions of the electromagnetic spectrum represented by each sensor. RapidEye and Pika both have bands from the visible to the NIR, whereas Landsat also contains bands, for our purposes, into the SWIR, which does have a change in reflectance in the event of vegetation stress. RapidEye and Pika also have bands covering the red edge portion of the spectrum, which has commonly been used in vegetation stress studies while Landsat does not.

It was surprising to see in the sensitivity analysis that there were 140 pixels where no RapidEye pixels detected any stress indicators where a Landsat pixel contained at least one (Fig. 6). This can most likely be attributed to the different portions of the electromagnetic spectrum each sensor covers. 125 of the 147 stress indicators (85%) Landsat detected that RapidEye did not were in the NIR or SWIR bands. As mentioned above, Landsat has two SWIR bands that RapidEye does not. This explains the high number of SWIR stress indicators that RapidEye did not detect.

The large numbers of NIR differences, a band both sensors have, are most likely attributable to the different portions of the NIR that RapidEye and Landsat cover. The RapidEye NIR band covers the shorter NIR portion of the spectrum, from 760 to 850 nm. The Landsat 8 sensor's NIR band covers the longer NIR portion of the spectrum, from 850 to 880 nm. Earlier Landsat missions spanned a much larger portion of the NIR spectrum, from 770 to 900 nm, but the band was narrowed for the Landsat 8 mission to avoid the water absorption feature in the shorter wavelengths.[30] There is, as a result, no overlap between the Landsat and RapidEye NIR bands. Stresses might manifest differently in different portions of the NIR. This is a prime area for further research considering the differences in bandwidth and coverage across sensors.

This trend continued in the Pika/Landsat sensitivity analysis as well (Fig. 6). There were 105 pixels, 130 stress indicators, where Landsat detected a stress indicator and Pika detected none. 39 (30%) were visible anomalies, 51 (39.2%) were NIR anomalies, and 40 (30.8%) were SWIR anomalies. The Pika sensor, like RapidEye, does not have bands in the SWIR portion of the spectrum, which can account for the 40 indicators in this portion that Landsat detected that Pika did not. Unlike RapidEye, however, the Pika sensor has bands in the longer wavelengths of the NIR portion, so that the explanation for the differences with RapidEye does not apply to the Pika. This is true of the high number of visible anomalies that were undetected by Pika as well, as the two sensors have similar wavelength coverage in this portion of the spectrum. The ability of Landsat to detect stress indicators that the Pika did not might be the result of the superior radiometry of the Landsat OLI sensor. The OLI sensor has a much higher SNR, topping out at ∼350 in the blue band, making it potentially much more sensitive to spectral differences than the Pika, which has a maximum SNR of 198.[33]

4.3 *Limitations*

This study did not have reference data to determine the accuracy of using these stress indicators as actual locations of vegetation stress. There are some real-world instances, such as this one, that make obtaining reference data impossible. There were also site access issues due to much of the site being private property that required the permission of the landowners for access, which was not always available. We were able to confirm that some of the areas with detected anomalies were located in areas where anomalies would be expected, such as in saline seeps.

Figure 7 shows some similarities between the images and also areas that we would expect stress to be present. In the east-central portion of the image, there are rolling hills throughout the landscape. We expect vegetation to respond differently, spectrally, on the top of hills, where soil moisture is likely to be lower and vegetation, therefore, is likely to exhibit relative stress, as opposed to in valley bottoms. There is also evidence of anomalies in the western portion of the images between fields where limited vegetation is growing in fallow fields, which is

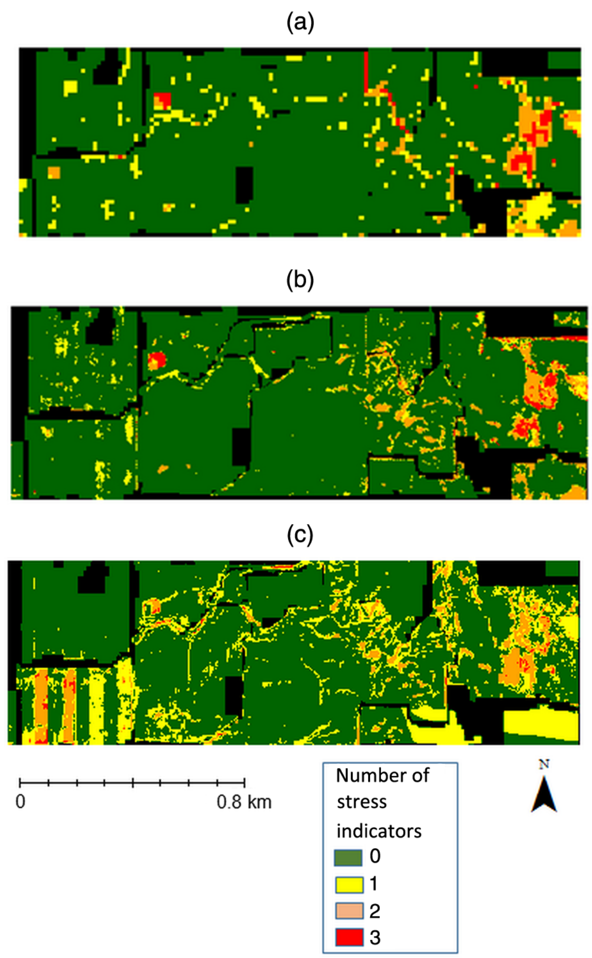

Fig. 7 (a) Landsat, (b) RapidEye, and (c) Pika images showing anomalous pixels in three areas of the study site.

also to be expected. The eastern-most portion of the image is a shrubby grassland with areas of bare ground, which is why anomalies are present in that region.

The black areas between these fields can be attributed to areas where we were trying to avoid edge effects and to areas where it was impossible to determine whether that portion of the field had been seeded or fallow in 2014, when the images were acquired.

5 Conclusion

The goal of this study was to highlight both the similarities and the differences among sensors with different characteristics. We did not use analysis techniques that take full advantage of the large number of bands in the hyperspectral sensor. Usually, hyperspectral and multispectral sensors are analyzed using different methods. In order to compare them, however, we used a band-by-band approach. This can hopefully provide guidance for managers as to tradeoffs among different sensors. The sensors in this study are representative of some of the sensor options that exist for vegetation stress monitoring. Cost, accessibility, and accuracy (Table 2) are all important considerations when determining which sensor is appropriate for the goals at hand. Landsat is free and relatively easy to access through the USGS Landsat archive. RapidEye, on the other hand, can become very costly very quickly if multiple images are needed for monitoring, but are relatively accessible by ordering them. Pika is a one-time cost. It does require flight planning when images are needed, and each flight is several hundred dollars, depending on the contractor and flight distances required. The accuracy of the sensors is also very important in a monitoring scheme. Landsat does have the largest pixel size, but as the sensitivity analysis indicates, it is able to detect stress indicators that occur over less than a full pixel. Landsat consistently detected stress indicators when only about $1/3$ of the RapidEye pixels within, the Landsat pixel detected them, and $1/6$ of the Pika pixels. Landsat also has the narrower NIR band and the additional SWIR band that detected stress indicators when the RapidEye and Pika did not. All of these are considerations land managers should take into account when planning a monitoring program. The sentinel 2 satellites might provide an excellent alternative, because they (1) have higher spatial resolution than Landsat in the relevant bands, (2) include coverage in the red edge, (3) include coverage in both areas of the NIR covered by RapidEye and Landsat, and (4) have coverage in the SWIR, which was important in our Landsat analysis.

This study also highlighted many opportunities for future research. For example: (1) an analysis of agreement as a function of standard deviation, (2) an analysis of whether agreement improved using band combinations or indices as opposed to a band-by-band approach, and (3) a similar study in a controlled environment to further explore one obstacle of this study, a lack of reference data, are all potential options.

Acknowledgments

This work was supported by the U.S. Department of Energy and the National Energy Technology Laboratory under Award No. DE-FC26-05NT42587. This report was prepared as an account of work sponsored by an agency of the United States Government. Neither the United States Government nor any agency thereof, nor any of its employees, makes any warranty, express or implied, or assumes any legal liability or responsibility for the accuracy, completeness, or usefulness of any information, apparatus, product, or process disclosed, or represents that its use would not infringe privately owned rights. Reference herein to any specific commercial product, process, or service by trade name, trademark, manufacturer, or otherwise does not necessarily constitute or imply its endorsement, recommendation, or favoring by the United States Government or any agency thereof. The views and opinions of authors expressed herein do not necessarily state or reflect those of the United States Government or any agency thereof.

References

1. M. S. Moran et al., "Estimating crop water deficit using the relation between surface-air temperature and spectral vegetation index," *Remote Sens. Environ.* **49**(3), 246–263 (1994).

2. G. J. Bellante et al., "Aerial detection of a simulated CO_2 leak from a geologic sequestration site using hyperspectral imagery," *Int. J. Greenhouse Gas Control* **13**, 124–137 (2013).
3. A. K. Tilling et al., "Remote sensing of nitrogen and water stress in wheat," *Field Crops Res.* **104**(1–3), 77–85 (2007).
4. N. M. Milton et al., "Arsenic- and selenium-induced changes in spectral reflectance and morphology of soybean plants," *Remote Sens. Environ.* **30**, 263–269 (1989).
5. A. Meddens, J. A. Hicke, and L. A. Vierling, "Evaluating the potential of multispectral imagery for mapping multiple stages of tree mortality," *Remote Sens. Environ.* **115**, 1632–1642 (2011).
6. K. L. Smith, M. D. Steven, and J. J. Colls, "Spectral responses of pot-grown plants to displacement of soil oxygen," *Int. J. Remote Sens.* **25**(25), 4395–4410 (2004).
7. G. A. Carter, "Responses of leaf spectral reflectance to plant stress," *Am. J. Bot.* **80**(3), 239–243 (1993).
8. G. A. Carter et al., "Response of leaf spectral reflectance in loblolly pine to increased atmospheric ozone and precipitation acidity," *J. Exp. Bot.* **43**(4), 577–584 (1992).
9. F. S. Chapin, "Integrated responses of plants to stress," *BioScience* **41**, 29–36 (1991).
10. G. A. Carter and R. L. Miller, "Early detection of plant stress by digital imaging within narrow stress-sensitive wavebands," *Remote Sens. Environ.* **50**(3), 295–302 (1994).
11. G. A. Carter, W. G. Cibula, and R. L. Miller, "Narrow-band reflectance imagery compared with thermal imagery for early detection of plant stress," *J. Plant Physiol.* **148**(5), 515–522 (1996).
12. E. B. Knipling, "Physical and physiological basis for the reflectance of visible and near-infrared radiation from vegetation," *Remote Sens. Environ.* **1**(3), 155–159 (1970).
13. M. Ashraf and P. J. C. Harris, "Photosynthesis under stressful environments: an overview," *Photosynthetica* **51**(2), 163–190 (2013).
14. G. A. Carter, "Primary and secondary effects of water content on the spectral reflectance of leaves," *Am. J. Bot.* **78**(7), 916–924 (1991).
15. L. Li, S. L. Ustin, and M. Lay, "Application of AVIRIS data in detection of oil-induced vegetation stress and cover change at Jornada, New Mexico," *Remote Sens. Environ.* **94**(1), 1–16 (2005).
16. D. N. H. Horler, M. Dockray, and J. Barber, "The red edge of plant leaf reflectance," *Int. J. Remote Sens.* **4**(2), 273–288 (1982).
17. G. A. Carter and A. K. Knapp, "Leaf optical properties in higher plants: linking spectral characteristics to stress and chlorophyll concentration," *Am. J. Bot.* **88**(4), 677–684 (2001).
18. J. E. Luther and A. L. Carroll, "Development of an index of balsam fir vigor by foliar spectral reflectance," *Remote Sens. Environ.* **69**(3), 241–252 (1999).
19. J. U. H. Eitel et al., "Active ground optical remote sensing for improved monitoring of seedling stress in nurseries," *Sensors* **10**(4), 2843–2850 (2010).
20. D. M. Gates et al., "Spectral properties of plants," *Appl. Opt.* **4**(1), 11–20 (1965).
21. C. L. Maynard et al., "Ecological site descriptions and remotely sensed imagery as a tool for rangeland evaluation," *Can. J. Remote Sens.* **33**(2), 109–115 (2007).
22. D. P. Roy et al., "Landsat-8: science and product vision for terrestrial global change research," *Remote Sens. Environ.* **145**, 154–172 (2014).
23. R. Reulke and H. Weichelt, "SNR evaluation of the RapidEye space-borne cameras," *Photogramm. Fernerkundung Geoinformation* **1**, 0029–0038 (2012).
24. Department of the Interior, Landsat 8 Data Users Handbook, https://landsat.usgs.gov/sites/default/files/documents/Landsat8DataUsersHandbook.pdf (29 March 2016).
25. Satellite Imaging Corporation, RapidEye Satellite Sensor, https://www.satimagingcorp.com/satellite-sensors/other-satellite-sensors/rapideye/.
26. Resonon, https://resonon.com/Products/imagers_pika_ii.html.
27. https://www.resonon.com.
28. Big Sky Carbon Sequestration Partnership, http://www.bigskyco2.org.
29. C. McCann et al., "Using landsat as a calibration target for radiometric correction of high resolution multi-swath hyperspectral imagery," *IEEE Trans. Remote Sens.* (2017). (in review).

30. K. L. Smith, M. D. Steven, and J. J. Colls, "Use of hyperspectral derivative ratios in the red-edge region to identify plant stress responses to gas leaks," *Remote Sens. Environ.* **92**(2), 207–217 (2004).
31. W. J. Ripple, "Asyptotic reflectance characteristics of grass vegetation," *Photogramm. Eng. Remote Sens.* **51**(12), 1915–1921 (1985).
32. NASA. Landsat Science, https://landsat.gsfc.nasa.gov/landsat-data-continuity-mission/ (20 November 2017).
33. J. R. Irons, J. L. Dwyer, and J. A. Barsi, "The next satellite: the Landsat data continuity mission," *Remote Sens. Environ.* **122**, 11–21 (2012).

Mikindra Morin received her BS degree in health science from Clemson University and her JD degree from the University of Arizona. She is a graduate student at Montana State University in the Land Resources and Environmental Sciences Department with an emphasis on spatial sciences. Her research focuses on monitoring vegetation stress using remotely sensed imagery.

Rick Lawrence received his BA degree in political science from Claremont McKenna College, his JD degree from Columbia University, and his MS and PhD degrees in forest resources from Oregon State University. He is a professor of remote sensing at Montana State University and director of its Spatial Sciences Center. His current research spans a wide range of applications related to natural resource management, from carbon sequestration, to crop and range issues, to forest and wildlife.

Kevin Repasky received his BE degree in mechanical engineering from Youngstown State University and his MS and PhD degrees in physics from Montana State University. He is a professor in the Electrical and Computer Engineering Department and an affiliate faculty member of the Physics Department at Montana State University and is a visiting scientist at the National Center for Atmospheric Research. His research interests include active and passive remote sensing instrument development and applications.

Tracy Sterling received her BS degree in agronomy from the University of Minnesota in 1983, her MS degree in horticulture from Michigan State University in 1985, and her PhD in botany and agronomy from the University of Wisconsin in 1988. She is a professor of plant physiology and a department head of the Land Resources and Environmental Sciences Department at Montana State University. Her research and teaching programs have centered on understanding how environmental, insect, and herbicide stress influence crop, and weed productivity.

Cooper McCann received his BS, MS, and PhD degrees in physics from Montana State University in 2004, 2015, and 2017 respectively. He has worked with high-power pulsed laser, nonlinear optics, and for several small startup optics companies. He is continuing his work with hyperspectral data in industry focusing on agricultural land management issues. His interests include hyperspectral imagery, "big data" processing, general optics, and teaching.

Scott Powell received his BA degree in biology from Macalester College, his MEM degree in resource ecology from Duke University, and his PhD in ecology from Montana State University. He is currently an assistant professor in the Department of Land Resources and Environmental Sciences at Montana State University. His research focuses on the use of geospatial data to characterize ecosystem and landscape processes, including quantification and monitoring of carbon sequestration.